



Methylene blue removal from aqueous solution by adsorption using *Jatropha* seed husks-activated carbon activated with KOH

Faheem Ahmed Qaid*, Ahmad Danial Azzahari, Abdul Hamid Yahaya, Rosiyah Yahya

Faculty of Science, Department of Chemistry, University of Malaya, Kuala Lumpur 50603, Malaysia, email: absifaheem@yahoo.com (F.A. Qaid)

Received 5 October 2014; Accepted 12 February 2015

ABSTRACT

The application of activated carbon (AC) from *Jatropha* seed husks for methylene blue (MB) adsorption from aqueous solution at room temperature was studied through batch experiments. The effects of adsorbent dosage, solution pH and initial concentration were studied. Adsorption increased as the adsorbent dosage, initial concentration and contact time increased with the highest adsorption obtained in basic conditions. The average pore diameter of the AC was 10.58 nm with surface area of 1262 m²/g, and total pore volume of 0.4992 cm³/g. Adsorption isotherm data fitted well with the Langmuir model, with a monolayer adsorption capacity of 250 mg/g. The adsorption kinetics obeyed a pseudo-second-order kinetic model. The negative values of free energy change (ΔG°) indicated that the adsorption of MB on AC16 is spontaneous. Also, the positive values of both entropy change (ΔS°) and enthalpy change (ΔH°) mean that the adsorbate has a random organization at the interface of the solid/solution and that the adsorption process was endothermic.

Keywords: Thermodynamics; Kinetics; Isotherm; *Jatropha* seed husks; Activated carbon; Methylene blue

1. Introduction

Dyes are an important source of water pollution where they are released from effluents of the cosmetics, textile, food processing, leather, paper, dye manufacturing industries, and dyeing [1]. Some dyes have been reported to be mutagenic and carcinogenic for aquatic organisms and humans [2,3]. Methylene blue (MB) has a cationic configuration that is frequently used for silk, wool, and dyeing cotton [4]. Exposure to contaminated wastewaters by MB will result in dyspnea, tachycardia,

vomiting, convulsions, cyanosis, methemoglobinemia, irritation to the gastrointestinal tract and skin, diarrhea, and nausea [5,6]. Therefore, the MB removal from industrial wastewaters becomes environmentally important. For this, various techniques like coagulation, chemical precipitation, membrane filtration, solvent extraction, reverse osmosis, and adsorption have been used for purification of the industrial effluents from MB [7]. Because of the fact that adsorption process stability is efficient to remove MB at any concentration with a relatively lower cost [6,7], many researchers reported that the adsorption is the best and

*Corresponding author.

the most commonly employed method in the treatment of wastewater. Many adsorbent surfaces have been used to remove MB, such as rice husk [8], activated carbon (AC) [9], glass fibers [10], peanut hull [11], neem leaf powder [12], Indian rosewood sawdust [13], fly ash [14], perlite [15], silica nanosheets derived from vermiculite [16], sand [17], cyclodextrin polymer [18], and natural phosphate [19].

AC has a large specific surface area, for that it is highly effective as adsorbents to some extent [20]. It is commonly used for the treatment systems of industrial wastewater. However, the major drawback is that its cost is relatively high. Therefore, many efforts have been focused to find cheaper substitutes, such as fly ash, coal, wool wastes, silica gel, wood wastes, agricultural wastes, clay materials, and sewage sludge [21]. The main aim of this research was to prepare and evaluate the AC from *Jatropha* seed husks adsorption capacity for the MB removal. The effects of AC dosage, solution pH, initial MB concentration, and contact time were investigated. In addition, equilibrium, kinetic, and thermodynamic models were employed to fit the data of experiments and the thermodynamic adsorption parameters were determined.

2. Material and methods

2.1. Adsorbent preparations and its characterization

A horizontal tube furnace was used to prepare ACs from *Jatropha* seed husks. Under optimized conditions, the activation temperature of 700°C, activation time of 1.5 h, and 30% w/v KOH concentration were chosen as parameters for preparing the AC designated as AC16. Specific surface areas (S_{BET}) of AC16 were measured using a surface analyzer (Sorpromatic Thermo Finnigan 1990, USA). The adsorbent pore structure was determined using the t-method. Surface morphology of the adsorbent was studied using field emission scanning electron microscopy (LEO 1,455 VP, England).

2.2. Adsorbate

MB, (28514 FLUKA— $\text{C}_{16}\text{H}_{18}\text{ClN}_3\text{S}\cdot x\text{H}_2\text{O}$) with molecular weight of 319.86 (purity $\geq 95\%$) and was supplied by Sigma-Aldrich (U.S.A.).

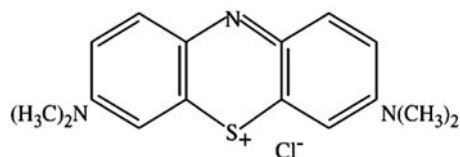


Fig. 1. Chemical structure of MB.

The MB structure is given by: Fig. 1.

The MB concentration in the aqueous solution was determined using UV–Visible spectrophotometry at λ_{max} of 669 nm. A stock solution of MB was prepared and subsequent required concentrations for each experiment were obtained by diluting the stock solution using distilled water.

2.3. Adsorption procedure

For every kinetic experiment, 25 mL of MB solution of known initial concentration and a 0.01 g sample of the AC were placed in a 30 mL stoppered sample bottle. The sample bottles were agitated at 150 rpm at room temperature for time intervals of 1, 2, 3, 4 ... 21 h in order to study the adsorption process. The adsorbent was separated from the mixture by filtration. The remaining MB concentration in the solution was determined using UV–Visible spectrophotometry. The percentage removal and the adsorbed amounts of MB onto the adsorbent (mg/g), q_e were calculated using Eqs. (1) and (2):

$$\% \text{ Removal} = \frac{C_0 - C_e}{C_0} \times 100 \quad (1)$$

$$q_e = \frac{(C_0 - C_e)V}{w} \quad (2)$$

where C_0 and C_e (mg/L) are the MB concentrations in solution at initial and at evolved time, respectively (mg/L); V is the solution volume of MB used in the adsorption experiment (L); and W is the dry adsorbent weight (g). The effects of solution pH, adsorbent dosage, and initial concentration were studied. In order to know the equilibrium time for maximum adsorption, the MB adsorption on AC16 was studied within sufficient range of contact time. In this study, the contact time of MB removal was performed at different intervals ranging from 1 to 21 h. For effect of solution pH, about 0.01 g of the dry AC16 was put into each sample bottle separately. Each bottle was added with 25 mL of MB solution for 50 mg/L. Each solution pH was adjusted by hydrochloric acid (HCl) and/or sodium hydroxide (NaOH) prepared in 0.1 N solution.

3. Results and discussion

3.1. Effect of contact time

The adsorbed amount of dye (mg/g) increased with increase in contact time until it reached

equilibrium. As shown in Fig. 2, the required time of the equilibrium for the MB adsorption on AC16 ranged from 6 to 16 h. The increase of initial MB concentration from 10 to 50 mg/L at equilibrium led to the increase in the adsorption capacity from 24.99 to 103.57 mg/g. For this, the initial concentration of dye supplies the driving force, which is necessary to overcome the resistances to the mass MB transfer between the two phases (aqueous and solid) [22].

3.2. Effect of solution pH

The solution pH is a very important parameter for controlling the dye adsorption on the adsorbent surface [23]. Fig. 3 shows that the increase of solution pH of MB from 2.0 to 6.0 sharply increased the amount of MB adsorbed. However, above pH 6.0, the adsorption rate slightly decreased. MB is an electron donor; so, when the solution pH becomes greater than the pK_a of the MB ($pH > pK_a$), it becomes an ion ($MB \text{ } pK_a < 1$). Therefore, the increase in adsorption process when pK_a is lower than the solution pH ($pH > 1$) is due to the attractive forces between the positive groups on the surface of AC16 and anions of MB. As seen in Fig. 3, at solution pH above 6 until 10, the adsorption processes were less strong than low values of solution pH; this is because of the competition from OH^- ions which are present on the adsorbent surface, which can decrease removal of MB ions from the solution. The

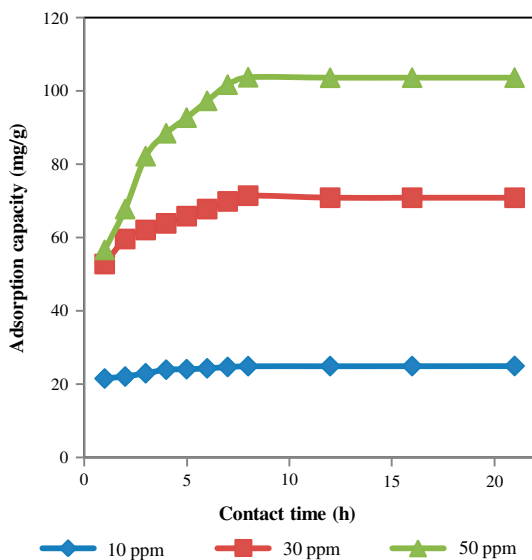


Fig. 2. Effect of contact time on MB adsorption process by AC16 (initial MB concentrations \blacklozenge 10, \blacksquare 30, and \blacktriangle 50 mg/L). Conditions: adsorbent dosage = 0.01 g/25 mL, temperature = 298 K, normal solution pH, and rpm = 150.

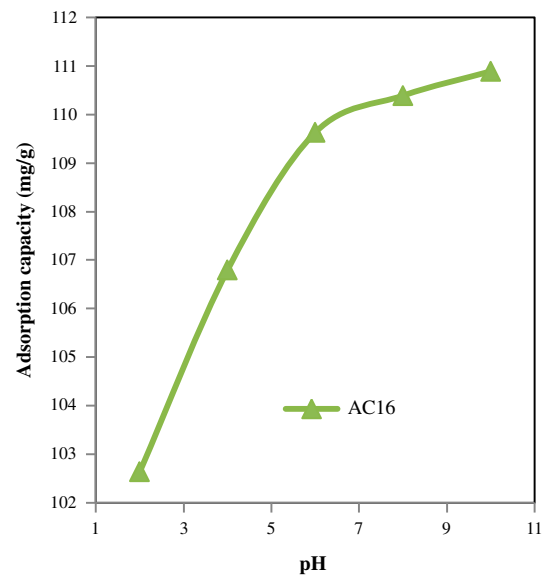


Fig. 3. Effect of solution pH values on the adsorption capacities of AC16 for 50 mg/L MB concentration. Conditions: contact time = 6 h, temperature = 298 K, agitation speed = 150 rpm, and adsorbent dosage = 0.01 g/25 mL.

optimum pH for the MB removal from aqueous solution by AC16 was found to be 9.5.

3.3. Effective dosage of AC16 adsorbent

The effect of AC16 dosage is shown in Fig. 4. The percentage of removal color for MB increased rapidly from 80.82 to 99.24% with the amount of added AC16

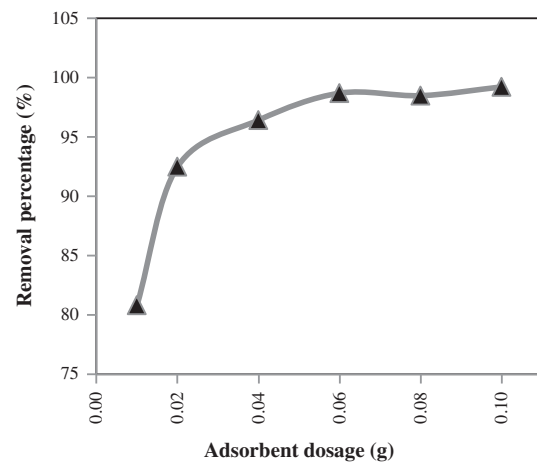


Fig. 4. Effect of adsorbent dosage on the MB removal by AC16. Conditions: contact time 150 min, temperature = 298 K, normal solution pH, and agitation speed = 150 rpm, initial MB concentration of 50 mg/L.

shavings from 0.01 to 0.10 g. The removal percentage increased with increase in dosage of AC16. However, at high adsorbent dosage (after 0.06 g), the removal rate of MB remained constant. This may be ascribed to the fact that there are many sites that are available through the adsorption process leading to a low ratio between the MB molecules to adsorbent dosage. The optimum adsorbent dosage for the MB removal from aqueous solution by AC16 was 0.06 g/L.

3.4. Effect of initial concentration of MB

Fig. 5(a) shows that the adsorption capacity of AC16 increased from 54.15 to 215.40 mg/g with an increase in the initial concentrations of MB solution from 30 to 200 mg/L. This can be explained by the fact that the driving force of mass transfer increases with the increase of initial concentration MB when it passes to the particle surface from the solution [24]. Also, the improvement of the adsorption capacity of the adsorbents might be explained by the fact that more molecules of adsorbate are available to surround the adsorbent surface at high concentration. On the other hand, as shown in Fig. 5(b), the percentage removal decreased with an increase in the solution concentrations above 50 mg/L. The decrease of the adsorption with an increase in the initial solution concentration may be due to the accumulation of molecules of MB caused by competition of the molecules to enter the pores on the adsorbent surface. Also, the decrease of vacant adsorption sites in the surface area is one of the reasons for the decrease because the ratio between MB molecules to the adsorbent dosage increases with the increase of the initial concentration.

3.5. Adsorption isotherms

Both Langmuir and Freundlich isotherms were employed in this work. For the Langmuir isotherm, the model assumes that the removal of adsorbate occurs on a homogeneous surface at uniform adsorption energies and without any interaction between the molecules of adsorbate on the surface of the carbon. The Freundlich isotherm model, unlike that of Langmuir, assumes that the adsorbate uptake happens on heterogeneous surface sites. The linear forms of the Langmuir and Freundlich isotherm model equations are given in Eqs. (3) and (4), respectively, [25,26]:

$$\frac{C_e}{q_e} = \frac{1}{q_{\max} K_L} + \frac{C_e}{q_{\max}} \quad (3)$$

where q_e (mg/g) is the amount of adsorbate adsorbed and C_e (mg/L) is the equilibrium adsorbate concentration. The b and q_{\max} are the Langmuir constants for adsorption energy and complete monolayer coverage at the maximum adsorption capacity of the surface.

$$\log q_e = \log K_F + \frac{1}{n} \log C_e \quad (4)$$

where q_e (mg/g) is the amount adsorbed of adsorbate and C_e (mg/L) represents the remaining concentration of adsorbate at equilibrium (mg/L); n and K_F represents the constants of the Freundlich isotherm for the intensity and adsorption capacity, respectively.

Fig. 6(a) and (b) illustrates the adsorption isotherms of the experiment by Langmuir and Freundlich

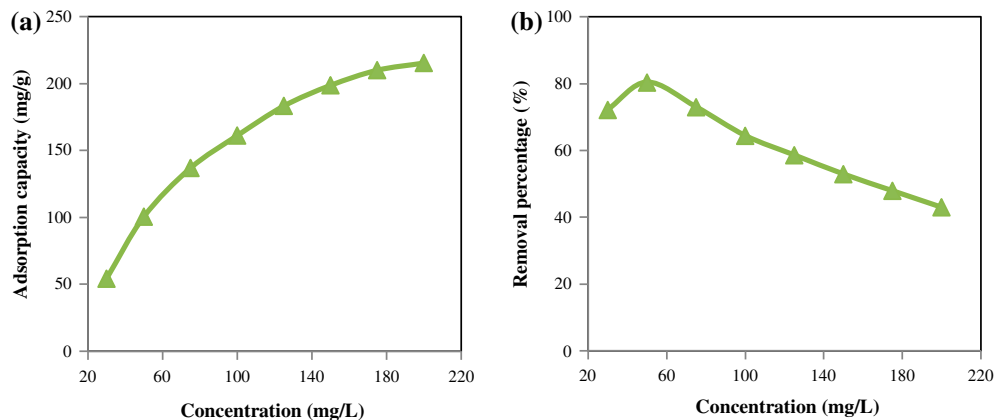


Fig. 5. Effect of different initial concentrations of MB solution on (a) adsorption capacity of AC16 and (b) percentage of removal of MB by AC16. Conditions: adsorbent dose = 0.01 g/25 mL, contact time = 150 min, temperature = 298 K, and agitation speed = 150 rpm.

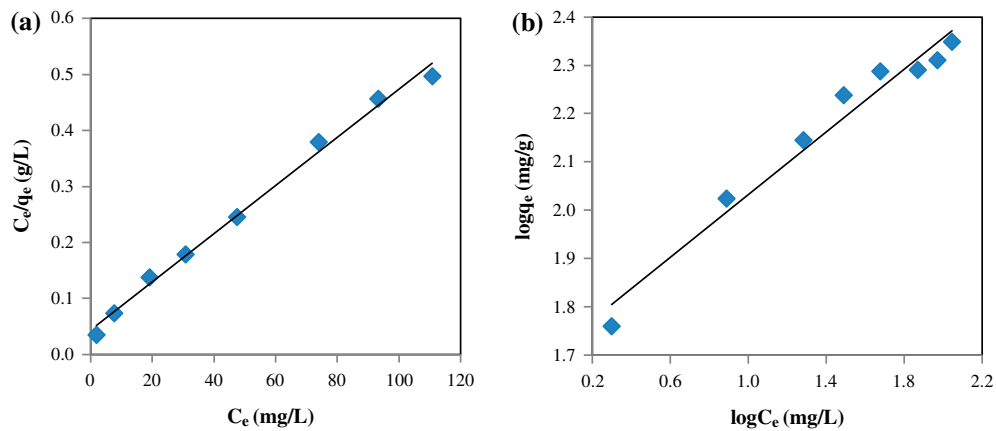


Fig. 6. (a) Langmuir isotherm plot and (b) Freundlich isotherm plot of MB adsorption on AC16 as adsorbent.

models. Both isotherm models fitted well with the experimental data. All the parameter values of the Langmuir and Freundlich models and their correlation

Table 1

Parameters of Langmuir and Freundlich models for the adsorption isotherm of MB on AC (AC16) at room temperature

Adsorbent	Langmuir			Freundlich			
	q_{max}	K_L	R^2	K_F	$1/n$	n	R^2
AC16	250	0.0952	0.993	51.05	0.324	3.086	0.966

coefficients are shown in Table 1. In the Freundlich isotherms, K_L value was between zero and one indicating the adsorption energy was favorable. In the Freundlich isotherms, the $1/n$ value is between 0 and 1 and the K_F value is high, which means the MB adsorption on the AC16 is favorable. However, the coefficient correlations of the Langmuir isotherm are higher than those of the Freundlich model. For this, the description of adsorption isotherm by Langmuir is better than by Freundlich isotherm. Therefore, the adsorption of MB is more likely to occur by the monolayer adsorption process on the surface of AC16.

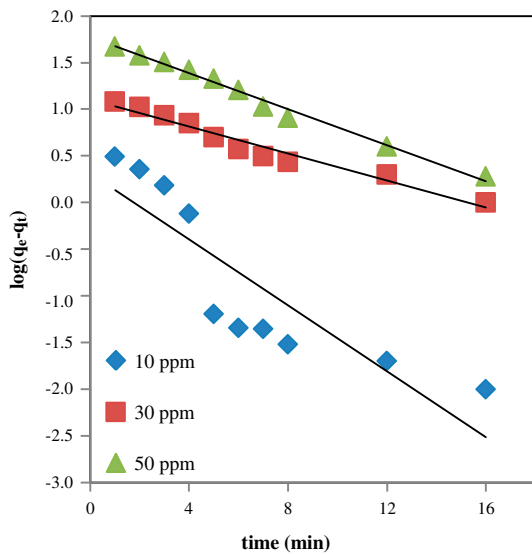


Fig. 7. Pseudo-first-order kinetics by linear method for the MB adsorption on adsorbents AC16. Condition: adsorbent dosage = 0.01 g/25 mL, normal pH, and agitation speed = 150 rpm.

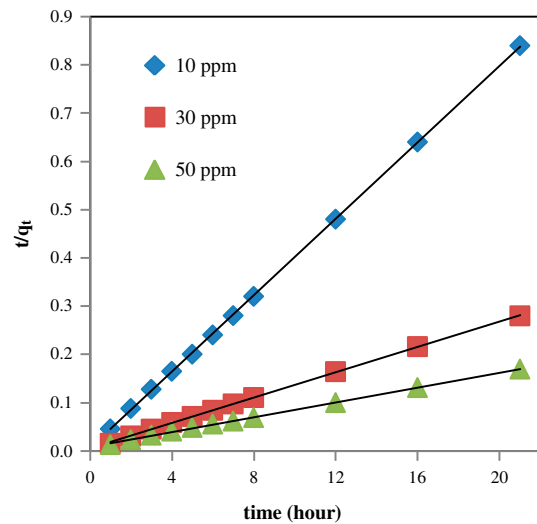


Fig. 8. Plot of pseudo-second-order kinetic by linear method for the MB adsorption on adsorbent AC16. Conditions: adsorbent dose = 0.01 g/25 mL, normal pH, and agitation speed = 150 rpm.

Table 2
Adsorption kinetic parameters of MB onto AC16

Adsorbent	C ₀ (mg/L)	q _{e,exp.} (mg/g)	First order			Second order		
			q _{e,cal.} (mg/g)	K ₁	R ²	q _{e,cal.} (mg/g)	K ₂	R ²
AC16	10	24.99	2.048	0.40694	0.7613	25.25	0.2904	0.9999
	30	74.99	12.73	0.16696	0.9563	75.76	0.033508	0.9998
	50	123.8	58.95	0.22177	0.9894	129.9	0.006894	0.9991

3.6. Adsorption kinetics

Adsorption kinetics is used to understand the adsorption process. Among the many kinetic models, there are three models which were used in this study to fit the experimental data. The linear form of the pseudo-first-order kinetic model equation is given as in Eq. (5):

$$\log(q_e - q_t) = \log q_e - k_1 \frac{t}{2.303} \tag{5}$$

where q_e is the MB concentration adsorbed at equilibrium, q_t is the MB concentration adsorbed at time t, and k₁ (min⁻¹) is the pseudo-first-order rate constant.

The linear form of the pseudo-second-order equation is given as in Eq. (6):

$$\frac{t}{q_t} = \frac{1}{k_2 q_e^2} + \frac{t}{q_e} \tag{6}$$

where k₂ (g/mg min) and q_e are the pseudo-second-order rate constant and MB concentration adsorbed at equilibrium, respectively.

The intraparticle diffusion model is an empirical model, which assumes that the adsorption capacity varies with t^{1/2} adsorption capacity [27]. The intraparticle diffusion model equation is expressed as follows:

$$q_t = k_{dif} t^{1/2} + C \tag{7}$$

where the intraparticle diffusion kinetic parameters are K_{dif} (mg/g h)^{1/2} and C.

Table 3
The intraparticle diffusion constants at different initial concentrations

Adsorbent	C ₀ (mg/L)	Intraparticle diffusion		
		K _p (mg/g min ^{-1/2})	C	R ²
AC16	10	1.7471	20.492	0.9039
	30	6.6848	52.709	0.9448
	50	18.458	58.272	0.9975

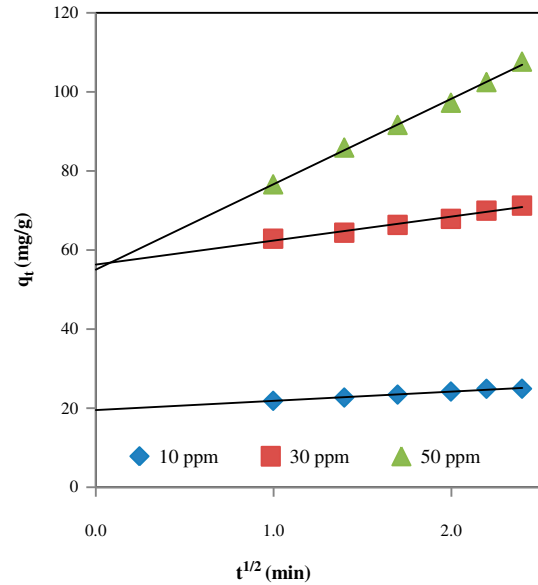


Fig. 9. Intraparticle diffusion kinetic model by linear method for the adsorption of MB on AC16. Conditions: adsorbent dosage = 0.01 g/25 ml, normal pH, and agitation speed = 150 rpm.

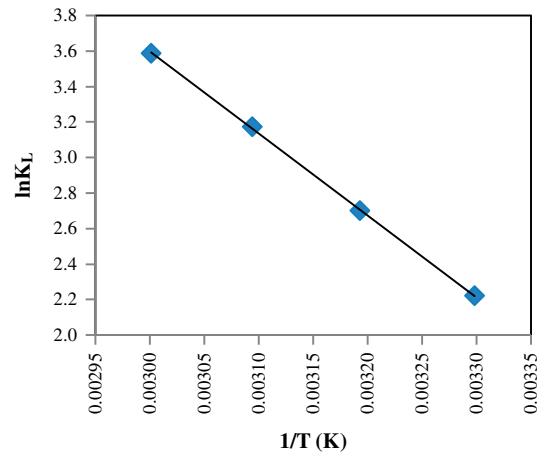


Fig. 10. Plot of ln K_d vs. 1/T for estimation of standard enthalpy and entropy change of the adsorption of MB on AC16.

Table 4

Adsorbate distribution coefficients, correlation coefficient, and thermodynamic parameters of adsorption of MB on AC16 at different temperatures

Adsorbent	K_d				ΔG°				ΔH°	ΔS°	R^2
	30°C	40°C	50°C	60°C	30°C	40°C	50°C	60°C			
AC16	9.22	14.9	23.9	36.12	-5.59	-7.03	-8.53	-9.94	38.38	0.15	0.99

The experimental data of the pseudo-first-order and pseudo-second-order kinetic model at different initial concentrations are shown in Figs. 7 and 8, respectively. All the constant parameters are shown in Table 2. The values of correlation coefficient (R^2) for the pseudo-second-order rate equation were much higher than those of the pseudo-first-order model. The rate constant values of the pseudo-second-order (k_2) generally decreased with the increase of the initial concentration. The increase in the concentration of MB solution may reduce the MB diffusion in the boundary layer between the liquid and the solid adsorbent. Also, the values of the calculated adsorption capacity of the pseudo-second-order are close to the experimental values, q_{exp} than the calculated values of the pseudo-first-order. For this, the MB adsorption onto AC16 could be sensibly described by the pseudo-second-order model [28].

The parameters of the intraparticle diffusion kinetic model and the correlation coefficients are presented in Table 3. The plots of q_t vs. $t^{1/2}$ are shown in Fig. 9 for the adsorption of MB onto AC16 at different initial MB concentrations. It is observed that the straight lines did not pass through the origin, the intercept (C) was more than zero, and the R^2 values were not much higher. For this, the intraparticle diffusion does not control the adsorbate transport from the bulk of the solution to adsorbents AC16 [29].

3.7. Adsorption thermodynamics

The thermodynamic parameter values at different temperatures were calculated by using the following equations [30,31]:

$$K_d = q_e/C_e \quad (8)$$

$$\Delta G^\circ = -RT \ln K_d \quad (9)$$

$$\ln K_d = (\Delta S^\circ/R) - (\Delta H^\circ/RT) \quad (10)$$

where, K_d indicates the ratio between the equilibrium concentrations of the MB in solution and on the adsorbent, C_0 and C_e are the equilibrium concentrations of

MB on AC16 (mg/L) and in the solution (mg/L), respectively. R is the gas universal constant (8.314 J/mol K) and T is the temperature in Kelvin. At different temperatures, ΔG° was calculated by Eq. (9) using the values of $\ln K_d$. From Fig. 10, ΔS° and ΔH° values can be calculated from the intercept and slope of the linear plot of $\ln K_d$ against $1/T$, respectively. As shown in Table 4, all values of ΔG° are negative, indicating that the adsorption process of MB on AC16 was spontaneous. Moreover, the negative values of ΔG° increase as the temperature increases; this indicates that the adsorption process at high temperature is spontaneous [32] and more efficient. The value of ΔH° is positive, indicating that the adsorption process of the MB on AC16 was endothermic. The ΔS° value of adsorption process for MB on AC16 was also positive, indicating the randomness at the interface of the adsorbent–solution.

4. Conclusion

Jatropha seed husks were used as a raw material for the preparation of AC (AC16). The adsorption capacity of MB on AC16 increased with increase in contact time, solution pH, and initial concentration. The Langmuir and Freundlich isotherm models were used to evaluate of the mechanism of adsorption on the AC16 surface. It was found that the Langmuir model offer a better fit than the Freundlich model for adsorption of MB on AC16. Amongst the pseudo-first-order, pseudo-second-order, and intraparticle diffusion kinetic models used to analyze the adsorption kinetics, the pseudo-second-order equation was the best to describe the kinetic experimental data. The values of the thermodynamic parameters, i.e. ΔH° , ΔS° , and ΔG° indicated that the adsorption process on the AC16 surface was spontaneous, endothermic, and random at the interface of the adsorbent–solution.

Acknowledgments

The authors wish to express their gratitude to UM for the financial support through the Grant PV045-2012A which made this work possible.

References

- [1] A. Bhatnagar, A.K. Jain, A comparative adsorption study with different industrial wastes as adsorbents for the removal of cationic dyes from water, *J. Colloid Interface Sci.* 281 (2005) 49–55.
- [2] K.C. Chen, J.Y. Wu, C.C. Huang, Y.M. Liang, S.C.J. Hwang, Decolorization of azo dye using PVA-immobilized microorganisms, *J. Biotechnol.* 101 (2003) 241–252.
- [3] R. Gong, Y. Ding, M. Li, C. Yang, H. Liu, Y. Sun, Utilization of powdered peanut hull as biosorbent for removal of anionic dyes from aqueous solution, *Dyes Pigm.* 64 (2005) 187–192.
- [4] A.M. Vargas, A.L. Cazetta, M.H. Kunita, T.L. Silva, V.C. Almeida, Adsorption of methylene blue on activated carbon produced from flamboyant pods (*Delonix regia*): Study of adsorption isotherms and kinetic models, *Chem. Eng. J.* 168 (2011) 722–730.
- [5] S. Senthilkumaar, P.R. Varadarajan, K. Porkodi, C.V. Subbhuraam, Adsorption of methylene blue onto jute fiber carbon: Kinetics and equilibrium studies, *J. Colloid Interface Sci.* 284 (2005) 78–82.
- [6] H. Deng, J. Lu, G. Li, G. Zhang, X. Wang, Adsorption of methylene blue on adsorbent materials produced from cotton stalk, *Chem. Eng. J.* 172 (2011) 326–334.
- [7] Y. Liu, Y. Zheng, A. Wang, Enhanced adsorption of Methylene Blue from aqueous solution by chitosan-g-poly (acrylic acid)/vermiculite hydrogel composites, *J. Environ. Sci.* 22 (2010) 486–493.
- [8] V. Vadivelan, K.V. Kumar, Equilibrium, kinetics, mechanism, and process design for the sorption of methylene blue onto rice husk, *J. Colloid Interface Sci.* 286 (2005) 90–100.
- [9] E.N. El Qada, S.J. Allen, G.M. Walker, Adsorption of basic dyes from aqueous solution onto activated carbons, *Chem. Eng. J.* 135 (2008) 174–184.
- [10] S. Chakrabarti, B.K. Dutta, On the adsorption and diffusion of Methylene Blue in glass fibers, *J. Colloid Interface Sci.* 286 (2005) 807–811.
- [11] R. Gong, Y. Sun, J. Chen, H. Liu, C. Yang, Effect of chemical modification on dye adsorption capacity of peanut hull, *Dyes Pigm.* 67 (2005) 175–181.
- [12] K.G. Bhattacharyya, A. Sharma, Kinetics and thermodynamics of Methylene Blue adsorption on neem (*Azadirachta indica*) leaf powder, *Dyes Pigm.* 65 (2005) 51–59.
- [13] V.K. Garg, M. Amita, R. Kumar, R. Gupta, Basic dye (methylene blue) removal from simulated wastewater by adsorption using Indian Rosewood sawdust: A timber industry waste, *Dyes Pigm.* 63 (2004) 243–250.
- [14] L. Wang, J. Zhang, A. Wang, Removal of methylene blue from aqueous solution using chitosan-g-poly (acrylic acid)/montmorillonite superadsorbent nanocomposite, *Colloids Surf. A* 322 (2008) 47–53.
- [15] M. Doan, M. Alkan, A. Türkyilmaz, Y. Özdemir, Kinetics and mechanism of removal of methylene blue by adsorption onto perlite, *J. Hazard. Mater.* 109 (2004) 141–148.
- [16] M. Zhao, Z. Tang, P. Liu, Removal of methylene blue from aqueous solution with silica nano-sheets derived from vermiculite, *J. Hazard. Mater.* 158 (2008) 43–51.
- [17] S.B. Bukallah, M.A. Rauf, S.S. Alali, Removal of Methylene Blue from aqueous solution by adsorption on sand, *Dyes Pigm.* 74 (2007) 85–87.
- [18] G. Crini, Kinetic and equilibrium studies on the removal of cationic dyes from aqueous solution by adsorption onto a cyclodextrin polymer, *Dyes Pigm.* 77 (2008) 415–426.
- [19] N. Barka, A. Assabane, A. Nounah, L. Laanab, Y. Ichou, Removal of textile dyes from aqueous solutions by natural phosphate as a new adsorbent, *Desalination* 235 (2009) 264–275.
- [20] V. Yağın, V. Sevinc, Studies of the surface area and porosity of activated carbons prepared from rice husks, *Carbon* 38 (2000) 1943–1945.
- [21] H. Aydın, G. Baysal, Adsorption of acid dyes in aqueous solutions by shells of bittim (*Pistacia khinjuk* Stocks), *Desalination* 196 (2006) 248–259.
- [22] D. Mohan, K.P. Singh, V.K. Singh, Trivalent chromium removal from wastewater using low cost activated carbon derived from agricultural waste material and activated carbon fabric cloth, *J. Hazard. Mater.* 135 (2006) 280–295.
- [23] M. Sarioglu, U.A. Atay, Removal of methylene blue by using biosolid, *Global Nest J.* 8 (2006) 113–120.
- [24] A. Kuleyin, Removal of phenol and 4-chlorophenol by surfactant-modified natural zeolite, *J. Hazard. Mater.* 144 (2007) 307–315.
- [25] I. Langmuir, The constitution and fundamental properties of solids and liquids. Part I. solids, *J. Am. Chem. Soc.* 38 (1916) 2221–2295.
- [26] H.M.F. Freundlich, Over the adsorption in solution, *J. Phys. Chem.* 57 (1906) 1100–1107.
- [27] C. Theivarasu, S. Mylsamy, Equilibrium and kinetic adsorption studies of Rhodamine-B from aqueous solutions using cocoa (*Theobroma cacao*) shell as a new adsorbent, *Int. J. Eng. Sci. Technol.* 2 (2010) 6284–6292.
- [28] N.K. Amin, Removal of reactive dye from aqueous solutions by adsorption onto activated carbons prepared from sugarcane bagasse pith, *Desalination* 223 (2008) 152–161.
- [29] B.H. Hameed, Evaluation of papaya seeds as a novel non-conventional low-cost adsorbent for removal of methylene blue, *J. Hazard. Mater.* 162 (2009) 939–944.
- [30] S. Karagoz, T. Tay, S. Ucar, M. Erdem, Activated carbons from waste biomass by sulfuric acid activation and their use on methylene blue adsorption, *Bioresour. Technol.* 99 (2008) 6214–6222.
- [31] M.A. Ashraf, M.A. Rehman, Y. Alias, I. Yusoff, Removal of Cd (II) onto *Raphanus sativus* peels biomass: Equilibrium, kinetics, and thermodynamics, *Desalin. Water Treat.* 51 (2013) 4402–4412.
- [32] V.K. Gupta, A. Mittal, V. Gajbe, Adsorption and desorption studies of a water soluble dye, Quinoline Yellow, using waste materials, *J. Colloid Interface Sci.* 284 (2005) 89–98.